Virus Research 179 (2014) 93–101

Contents lists available at ScienceDirect

Virus Research

journal homepage: www.elsevier.com/locate/virusres

Changes in immune cell populations in the periphery and liver of GBV-B-infected and convalescent tamarins (*Saguinus labiatus*)

Simon P. Hood[a,1], Edward T. Mee[a], Hannah Perkins[b], Ori Bowen[a], Jessica M. Dale[a,2], Neil M. Almond[a], Peter Karayiannis[c,3], Helen Bright[b], Neil J. Berry[a,*], Nicola J. Rose[a,*]

[a] *Division of Virology, National Institute for Biological Standards and Control, Medicines and Healthcare products Regulatory Agency, Blanche Lane, South Mimms, Potters Bar, Hertfordshire EN6 3QG, UK*
[b] *Internal Medicine Research Unit, Pfizer Research and Development, Sandwich, Kent CT13 9NJ, UK*
[c] *Hepatology and Gastroenterology Section, Department of Medicine, Imperial College London, Variety Wing Floor D, St. Mary's Campus, Norfolk Place, London W2 1PG, UK*

ARTICLE INFO

Article history:
Received 5 July 2013
Received in revised form 3 November 2013
Accepted 7 November 2013
Available online 15 November 2013

Keywords:
Acute viral hepatitis
Immune cell
GBV-B

ABSTRACT

Flaviviruses related to hepatitis C virus (HCV) in suitable animal models may provide further insight into the role that cellular immunity contributes to spontaneous clearance of HCV. We characterised changes in lymphocyte populations in tamarins with an acute GBV-B infection, a hepatitis virus of the flaviviridae. Major immune cell populations were monitored in peripheral and intra-hepatic lymphocytes at high viraemia or following a period when peripheral virus was no longer detected. Limited changes in major lymphocyte populations were apparent during high viraemia; however, the proportions of $CD3^+$ lymphocytes decreased and $CD20^+$ lymphocytes increased once peripheral viraemia became undetectable. Intrahepatic lymphocyte populations increased at both time points post-infection. Distinct expression patterns of PD-1, a marker of T-cell activation, were observed on peripheral and hepatic lymphocytes; notably there was elevated PD-1 expression on hepatic $CD4^+$ T-cells during high viraemia, suggesting an activated phenotype, which decreased following clearance of peripheral viraemia. At times when peripheral vRNA was not detected, suggesting viral clearance, we were able to readily detect GBV-B RNA in the liver, indicative of long-term virus replication. This study is the first description of changes in lymphocyte populations during GBV-B infection of tamarins and provides a foundation for more detailed investigations of the responses that contribute to the control of GBV-B infection.

1. Introduction

Hepatitis C virus (HCV) establishes a chronic infection in approximately 70% of infected individuals (Bowen and Walker, 2005; Chisari, 2005). The mechanisms by which the remainder eliminate detectable infection are not fully understood, though a vigorous multispecific $CD4^+$ and $CD8^+$ T-cell response is thought to contribute to viral clearance (Chang et al., 2001; Lechner et al., 2000; Thimme et al., 2001, 2002). Understanding the mechanisms underlying natural clearance is important both in designing immunotherapies and prophylactic vaccines. An inability to clear virus may, in part, be due to a failure of $CD4^+$ T-cells to support a sufficiently robust virus-specific $CD8^+$ T-cell response, implying that both T-cell subsets should be targeted in any therapeutic strategy (Chang et al., 2001). One obstacle to establishing the precise

Abbreviations: HCV, hepatitis C virus; GBV-B, GB virus B; PD-1, programmed death receptor-1; PD1-L1, programmed death receptor-1 ligand; CTLA4, cytotoxic T lymphocyte antigen-4; NS, non-structural; vRNA, viral ribonucleic acid; qRT-PCR, quantitative reverse transcriptase polymerase chain reaction; ge, genome equivalents; IVT, in vitro transcription; HBSS, Hank's balanced salt solution; EGTA, ethylene glycol tetraacetic acid; HEPES, 4-(2-hydroxyethyl)-1-piperazineethanesulfonic acid; RPMI, Roswell Park Memorial Institute medium; DMSO, dimethyl sulphoxide; FITC, Fluorescein isothiocyanate; PE, phycoerythrin; APC, allophycocyanin; IFN, interferon; MFI, median fluorescence intensity; IHL, intrahepatic lymphocytes; NK, natural killer; MHC, major histocompatibility complex.

* Corresponding authors at: Division of Virology, National Institute for Biological Standards and Control, Health Protection Agency, Blanche Lane, South Mimms, Potters Bar, Hertfordshire EN6 3QG, UK. Tel.: +44 01707 641000; fax: +44 01707 641060.

E-mail addresses: neil.berry@nibsc.org (N.J. Berry), nicola.rose@nibsc.org (N.J. Rose).

[1] Present address: John van Geest Cancer Research Centre, Nottingham Trent University, Clifton Campus, Nottingham NG11 8NS, UK.

[2] Present address: Faculty of Health and Wellbeing, Sheffield Hallam University, Howard Street, Sheffield S1 1WB, UK.

[3] Present address: St George's, University of London Medical School at University of Nicosia, 93, Agiou Nikolaou Street, Engomi, PO Box 24005, Nicosia 2408, Cyprus.

0168-1702
http://dx.doi.org/10.1016/j.virusres.2013.11.006

mechanism(s) of clearance is that many infections may be asymptomatic, hence the identification, monitoring and acquisition of samples from acutely HCV-infected patients is difficult.

Chimpanzees are susceptible to HCV however numerous constraints preclude their use. The infection of tamarins and marmosets with GBV-B represents an attractive surrogate model for the study of HCV infection in man (Beames et al., 2000, 2001; Lanford et al., 2003; Jacob et al., 2004). GBV-B is a flavivirus closely related to HCV and causes an acute self-limiting hepatitis: high viraemia is typically followed by viral clearance from the periphery within 18 weeks of infection (Beames et al., 2000, 2001; Bright et al., 2004). This model is applicable to the investigation of acute HCV pathogenesis, antiviral drug development and pre-clinical evaluation of candidate prophylactic vaccines (Butkiewicz et al., 2000; Beames et al., 2001; Bright et al., 2004; Jacob et al., 2004; Rijnbrand et al., 2005). Since GBV-B is most likely to have arisen in tamarins (Stapleton et al., 2011) we studied GBV-B-induced acute hepatitis in red-bellied tamarins to better understand changes in lymphocyte populations in both the periphery and liver, associated with the spontaneous resolution of the flavivirus infection. We explored changes in key cell populations, $CD4^+$, $CD8^+$ and $CD20^+$ cells, in the blood and the liver, between animals with high peripheral viraemia and those in a convalescence phase in which virus was undetectable in the periphery. Furthermore, since the mechanism of T-cell exhaustion has been implicated in persistence of several viruses, including HCV (Hofmeyer et al., 2011), we characterised the presence of the cell surface protein Programmed Death-1 (PD-1) on T-cells. Dysfunctional HCV-specific CD8 T-cells displaying up-regulated PD-1 and PD-1 ligand expression have been identified in the blood and liver of chronically infected individuals (Yao et al., 2007) and the reversal of T-cell exhaustion, evidenced by reduced PD-1 expression, has been associated with spontaneous clearance of chronic HCV infection (Raghuraman et al., 2012). In HCV-infected chimpanzees differences have been reported with higher intrahepatic PD-1 mRNA levels reported in chronically infected individuals by Rollier et al. (2007), while others have reported that PD-1 mRNA levels are not predictive of acute/chronic outcome of infection (Shin et al., 2013). We showed that in the convalescent phase of GBV-B infection a decrease in $CD3^+$ and a corresponding increase in $CD20^+$ lymphocytes occurred. Intrahepatic T- and B-lymphocyte populations were greater at high viraemia and convalescence than pre-infection.

A prerequisite to optimal exploitation of this model is a clear definition of the pathogenesis and naturally occurring host immune response against GBV-B in tamarins. We identified significant immune infiltration into the liver at high viraemia as well as in two of the four animals in the convalescent phase, concomitant with flares in serum ALT levels and vRNA was isolated from the livers of all animals, including those with undetectable peripheral viraemia. Antibodies against Core have only been reported for two tamarins (Nam et al., 2004; Bukh et al., 2008); our data on the limited immune responses to GBV-B NS3 are broadly consistent with the production of such antibodies in tamarins and marmosets (Beames et al., 2000; Lanford et al., 2003; Martin et al., 2003; Woollard et al., 2008).

This is the first description of the changes in a marker of T-cell activation/exhaustion on key immune cell populations in acute GBV-B infection of tamarins and the first report of an infection in the liver persisting when virus in no longer detected in the blood. These data provide a foundation for further immunological and pathological studies to dissect fully the mechanisms underlying natural viral clearance in this valuable surrogate model of acute HCV infection.

2. Materials and methods

2.1. Animals and virus inoculum

Eight purpose-bred red-bellied tamarins (*Saguinus labiatus*) were used. Animals were housed and maintained in accordance with the United Kingdom Animals (Scientific Procedures) Act 1986 and Home Office guidelines for care and maintenance of non-human primates. All animals were inoculated intravenously with 1×10^7 genome equivalents (ge) of GBV-B in serum. One group of four animals (animals W1, W2, W4, W11) was terminated at 6 weeks post-infection (wpi) and one group (animals W3, W5, V7, V8) was terminated following clearance of detectable virus from the periphery (approximately 24 wpi).

2.2. Quantification of GBV-B vRNA

To quantify GBV-B vRNA from the periphery, total RNA was extracted from 140 μl serum using the QIAamp Viral RNA Mini kit (Qiagen, UK). Core sequences were quantified in duplicate using the RNA Ultrasense One-step quantitative RT-PCR system. Primers 558F and 626R (Beames et al., 2000) were used at a concentration of 400 nM and 900 nM, respectively. The probe (5′ FAM-AGC GCG ATG CTC GGC CTC GTA AT-BHQ1 3′) was used at a concentration of 200 nM. Reverse transcription was performed at 50 °C for 15 min followed by amplification for 40 cycles (95 °C, 60 s; 62 °C, 30 s; 72 °C, 30 s). Standards to determine ge were derived from synthetic GBV-B RNA *in vitro* transcribed (IVT) from a plasmid (MEGAscript SP6; Ambion, USA). Serially diluted IVT RNA was quantified using a Poisson distribution; the limit of quantification was 10^2 ge/ml serum.

To quantify GBV-B vRNA from liver tissue, total RNA was extracted from a 0.5 cm^3 frozen section of liver in 1 ml RLT buffer (Qiagen RNeasy Mini Kit; Qiagen, UK). The tissue was homogenised using a 50 μM sterile Medicon unit (BD Biosciences) attached to a Medimachine (Dako), following the manufacturers' instructions. RNA was purified from the homogenate using the RNeasy Mini Kit (Qiagen) following the manufacturer's instructions. RNA was quantified and the concentration adjusted to 0.2 μg/μl. vRNA was quantified as described for serum vRNA levels and titres expressed per 400 ng total RNA (equating to approximately 10,000–15,000 cells). The limit of quantification was 7.6×10^{-2}/400 ng total RNA.

2.3. Quantification of serum liver enzymes

To indirectly assess liver damage, serum levels of alanine aminotransferase (ALT) and glutamate dehydrogenase (GLDH) were measured using a Kodak Ektachem automated analyser (Kodak Ltd. UK Suppliers, Orthochemical Diagnostics, Amersham, UK). Pre-infection samples were also assessed for each animal.

2.4. Isolation of intrahepatic lymphocytes (IHL)

Isolation of IHL from the liver retrieved at termination was performed on fresh tissue using adapted methods (Heydtmann et al., 2006; Nakamoto et al., 2008). The liver was washed at 37 °C by perfusion with 1 × HBSS (Life Technologies, UK) supplemented with 0.5 mM EGTA, 10 mM HEPES and 50 μg/ml gentamycin. Hepatocytes were disaggregated by perfusion with collagenase solution (1 mg/ml collagenase type II [Life Technologies] in 1× HBSS). The capsule was removed and the liver finely diced and incubated in collagenase solution containing 1 μg/ml DN*ase*I (Sigma–Aldrich) at 37 °C for 1 h. IHL were gravity filtered through a 100 μm nylon mesh and purified over a Ficoll-Paque Plus (GE Healthcare, UK) density gradient. IHL were cryopreserved in 80% foetal calf serum (FCS) and 10% dimethylsulfoxide (DMSO) in 1× RPMI. IHL were available from one uninfected tamarin from a parallel study.

2.5. Analysis of T-cell and B-cell populations by flow cytometry

PBMC and IHL (available at termination only) were washed in 1× RPMI containing 1% FCS, pelleted and resuspended in CellWash (BD Biosciences, Oxford, UK) containing 1% FCS. Cells (3.5×10^5 cells

per well in a 96-well round-bottom plate) were stained with Aqua LIVE/DEAD Fixable stain (Life Technologies). For immunophenotyping, cells were stained with pre-titrated amounts of CD3-FITC (clone SP34, BD), CD4-PE-Cy7 (clone L200, BD), CD8-APC (clone LT8, AbD Serotec, Kidlington, UK) and CD20-PE (clone H299 (B1), Beckman Coulter, High Wycombe, UK). For analysis of PD-1, cells were stained with PD-1-PE (clone eBioJ105, eBioscience, Hatfield, UK) or PE-labelled isotype-matched control antibody with CD3, CD4 and CD8 as above. Following staining at room temperature for 30 min with agitation at 180 rpm, cells were washed twice, resuspended in 2% (v/v) formaldehyde in PBS and stored at 4 °C until analysis. Data acquisition was performed on a BD FACS CantoII system and analysed using BD FACS DIVA v6.1.2. Spectral compensation was applied using either BD CompBeads or single-stained cells.

2.6. Statistical analysis

Peripheral lymphocyte populations pre- and post-infection were compared using a two-tailed paired *t*-test. Differences in the absolute percentage of PD-1$^+$ lymphocytes were assessed by a two-tailed unpaired *t*-test. Differences in PD-1 expression levels (MFI) were assessed using a Mann–Whitney *U*-test. Analysis was performed using Prism v5.03 (GraphPad Software, CA, USA).

2.7. Analysis of IFN-γ production by IHL

To assess IFN-γ production in response to NS3 peptide stimulation, peptides (20mer with 10 residue overlap) spanning the GBV-B NS3 region (residue 941–1560; 61 peptides; Sigma–Aldrich) were used. Sufficient cells were available for analysis of six of the eight animals. Thawed IHL were resuspended in 10 ml R10 medium (1× RPMI containing 50 U/ml penicillin, 50 μg/ml streptomycin, 10% foetal calf serum; Life Technologies) and incubated for 4–6 h at 37 °C. Cells were pelleted and resuspended in RPMI; 5×10^6 cells/ml; 5×10^5 cells were aliquoted per well in a 96-well round bottomed plate. IHL were stimulated for 2 h at 37 °C with one of six peptide pools comprising 10 or 11 peptides, 2 μg/ml of anti-CD28 (clone CD28.2, BD) and 1 μg/ml of anti-CD49d (clone L25, BD). A combination of 50 ng/ml phorbol 12-myristate 13-acetate and 1 μM ionomycin (both Sigma–Aldrich) diluted in DMSO/RPMI was used as a positive control and 1% (v/v) DMSO was used as a negative control. Brefeldin A (Sigma–Aldrich) was added to all wells (final concentration, 10 μg/ml) and the plate was incubated overnight at 37 °C. Cells were stained with Aqua LIVE/DEAD Fixable stain and surface stained with PE-CD3, PE-Cy7-CD4 and APC-CD8 as before. Cells were fixed and permeabilised using Fix and Perm solution A (An der Grub, Vienna, Austria), washed and permeabilised using Fix and Perm solution B and incubated with either FITC-IFN-γ (clone 1-D1K, Mabtech, Sweden) or an isotype-matched control antibody at room temperature for 30 min with agitation at 180 rpm. Cells were washed twice with CellWash (BD), resuspended in 2% (v/v) formaldehyde in PBS and stored at 4 °C until analysis. Data were acquired as before. The gate for IFN-γ positive cells was set to exclude 99.9% of cells stained with the isotype-matched control antibody.

2.8. Histological analysis of liver tissue

Sections (4 μm) were cut from formalin-fixed, paraffin-embedded liver taken at termination. Sections were mounted onto glass slides, de-waxed using xylene and the tissue re-hydrated through an ethanol series. Haematoxylin and eosin (H&E) staining was performed, liver morphology was visualised by microscopy (Nikon Eclipse E400) and images captured using the Metaview software (Meta Imaging software, MDS Analytical Technologies Ltd., Berkshire, UK).

3. Results

3.1. Characterisation of GBV-B infection in red-bellied tamarins

Peripheral viral dynamics were broadly comparable early post-infection, with all animals becoming viremic 2 days post-infection and viral RNA levels reaching a plateau at 10^8–10^9 ge/ml serum 4–6 weeks post infection (wpi) (Fig. 1A). Levels of ALT flared slightly in all animals at the time of infection (full data set not shown). Four animals were terminated at 6 wpi when viraemia was in excess of 10^8 ge/ml in each animal. Intracellular vRNA was detected at high levels in liver tissue (>1×10^5 ge GBV-B/400 ng total RNA) in these animals (Fig. 1B) but no second flare in liver enzymes was detected (data not shown). Peripheral virus in the remaining four animals proceeded, with comparable viral loads to 10 wpi; thereafter two tamarins (W3 and V7) rapidly suppressed viral replication to undetectable levels (convalescence) by 14 wpi, one (V8) maintained viraemia until 18 wpi and viraemia was no longer detectable in the final animal (W5) by 21 wpi following a brief period of viral recrudescence between weeks 17 and 21. None of the four convalescent animals had detectable peripheral viraemia at the time of sacrifice (22 wpi (W3 and V7) and 23 wpi (W5 and V8) (Fig. 1A) but, significantly, liver-associated intracellular vRNA was detected in these animals at levels between 3×10^2 and 2×10^3 ge GBV-B/400 ng total RNA (Fig. 1B). In all four animals that were allowed to proceed to convalescence, a flare in ALT levels was observed around 5–6 wpi, concurrent with a minor drop in vRNA levels. Further enzyme flares were coincident with the initial decline in vRNA levels in all animals and the clearance of recrudesced virus from W5 (Fig. 1C).

3.2. Phenotyping of peripheral lymphocytes

Prior to infection, during the acute phase viraemia and after clearance of viraemia CD3$^+$ T-cells constituted the majority of the peripheral lymphocyte population in all animals (Fig. 2A). The remainder of the lymphocyte population was predominantly CD20$^+$ (Fig. 2B). A small proportion (typically <10%) of the lymphocyte population was CD3$^-$ CD20$^-$. At high viraemia three of the four tamarins had a small increase in the percentage of peripheral CD3$^+$ T-cells over pre-infection levels (Fig. 2A). This increase was associated with a trend towards increased CD4$^+$ T-cells and a significant decrease ($P = 0.015$) in CD8$^+$ T-cells (Fig. 2C and D). Changes in CD20$^+$ B-cells were less consistent (Fig. 2B).

In all four convalescent animals the percentage of CD3$^+$ T-cells was lower than ($P = 0.004$), while the percentage of CD20$^+$ B-cells was higher than ($P < 0.001$, Fig. 2A and B) that of the pre-infection samples. There was a trend towards a lower number of CD4$^+$ T-cells and a significantly greater number ($P = 0.035$) of CD8$^+$ T-cells (Fig. 2C and D). In all animals and at both time points tested the CD3$^+$ T-cell population was comprised primarily of CD4$^+$ cells (>67%) with the remainder of the CD3$^+$ population being predominantly CD8$^+$ (Fig. 2C and D).

3.3. Phenotyping of intrahepatic lymphocytes

Pre-infection IHL were not available thus data were compared to IHL from an unrelated naive tamarin, which were predominantly CD3$^-$ CD20$^-$ (Fig. 2A and B). By contrast, the IHL from the animals terminated at high viraemia had a greater percentage of CD3$^+$ and CD20$^+$ cells (Fig. 2A and B). The percentages of CD4$^+$ and CD8$^+$ T-cells in three of the tamarins were similar to those seen in the

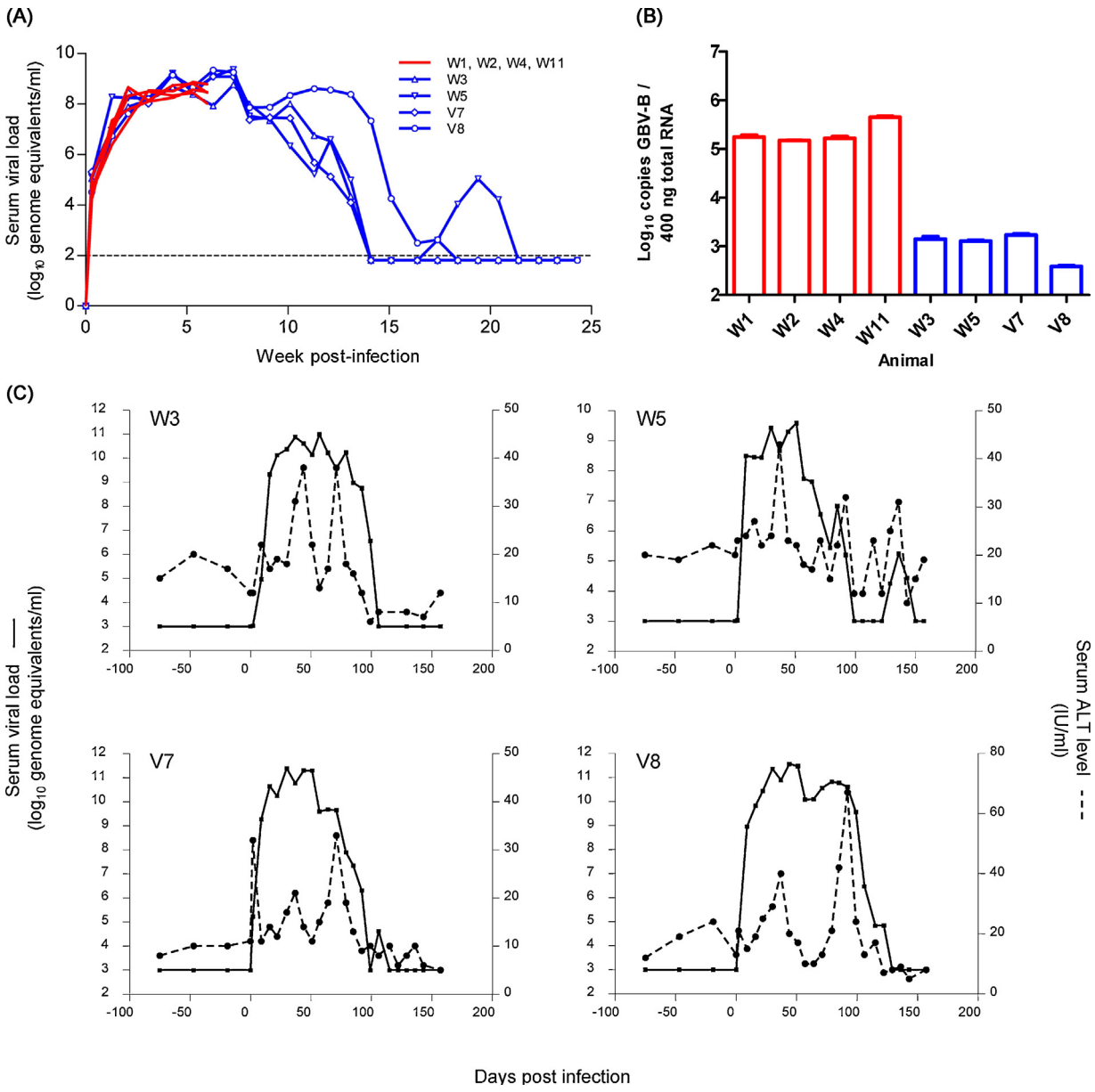

Fig. 1. Dynamics of GBV-B infection in red-bellied tamarins. (A) Viral load was monitored at weekly intervals in eight animals inoculated with 10^7 genome equivalents of infectious serum. Red lines represent animals terminated at 6 weeks post-infection. Animals displayed uniform viraemia profiles; hence symbols are omitted for clarity; blue lines indicate animals terminated in the convalescent phase. Dashed line indicates the limit of quantification of the qRT-PCR assay (100 ge/ml serum). (B) Viral load in the liver is presented as copies of virus per 400 ng total RNA (approximately 10,000–15,000 cells) for each animal. The limit of quantification was 7.6×10^{-2}/400 ng total RNA. Red bars indicate the animals terminated at 6 wpi; blue bars indicate the animals terminated in convalescence. (C) Changes in serum liver enzyme levels during infection are shown for the four animals which proceeded to convalescence. ALT levels (dotted line) are indicated for pre- and post-infection time points alongside peripheral viral load (solid line).

naive animal. The fourth animal (W2) had a higher percentage of $CD4^+$ T-cells and a lower percentage of $CD8^+$ T-cells (Fig. 2C and D). IHL isolated from the four convalescent tamarins exhibited two different patterns. The percentages of $CD3^+$ and $CD20^+$ cells in the IHL from tamarins W3 and V8 were similar to those seen in IHL from animals terminated at high viraemia while the percentage of $CD3^+$ and $CD20^+$ cells in tamarins W5 and V7 were comparable to those of the naive animal (Fig. 2A and B). In all four convalescent tamarins a significant proportion (≥40%) of the IHL fraction was $CD3^-$ $CD20^-$ (Fig. 2A). The percentage of $CD4^+$ and $CD8^+$ T-cells in three of the convalescent tamarins was similar to that seen in the naive animal. In contrast the fourth tamarin (W5) had a greater percentage of $CD8^+$ T-cells and a lower percentage of $CD4^+$ T-cells (Fig. 2C and D).

3.4. PD-1 expression on peripheral and intrahepatic $CD3^+$ T lymphocytes

Distinct patterns of PD-1 expression were observed on peripheral and intrahepatic lymphocytes. Peripheral PD-1 expression was typically uniform with a high frequency of cells (mean 76% of $CD3^+$ cells) staining with low intensity (mean MFI 1188), while PD-1 expression on IHL was more heterogeneous. Representative histograms and gating strategy are shown in Supplementary Fig. S1. A high percentage of both T-cell subsets in the periphery expressed PD-1 prior to infection (Fig. 3A). At high viraemia two tamarins (W1 and W2) retained a high percentage of PD-1-expressing $CD4^+$ and $CD8^+$ T-cells with levels comparable to those prior to infection. By contrast, of the remaining two tamarins one had a 2-fold

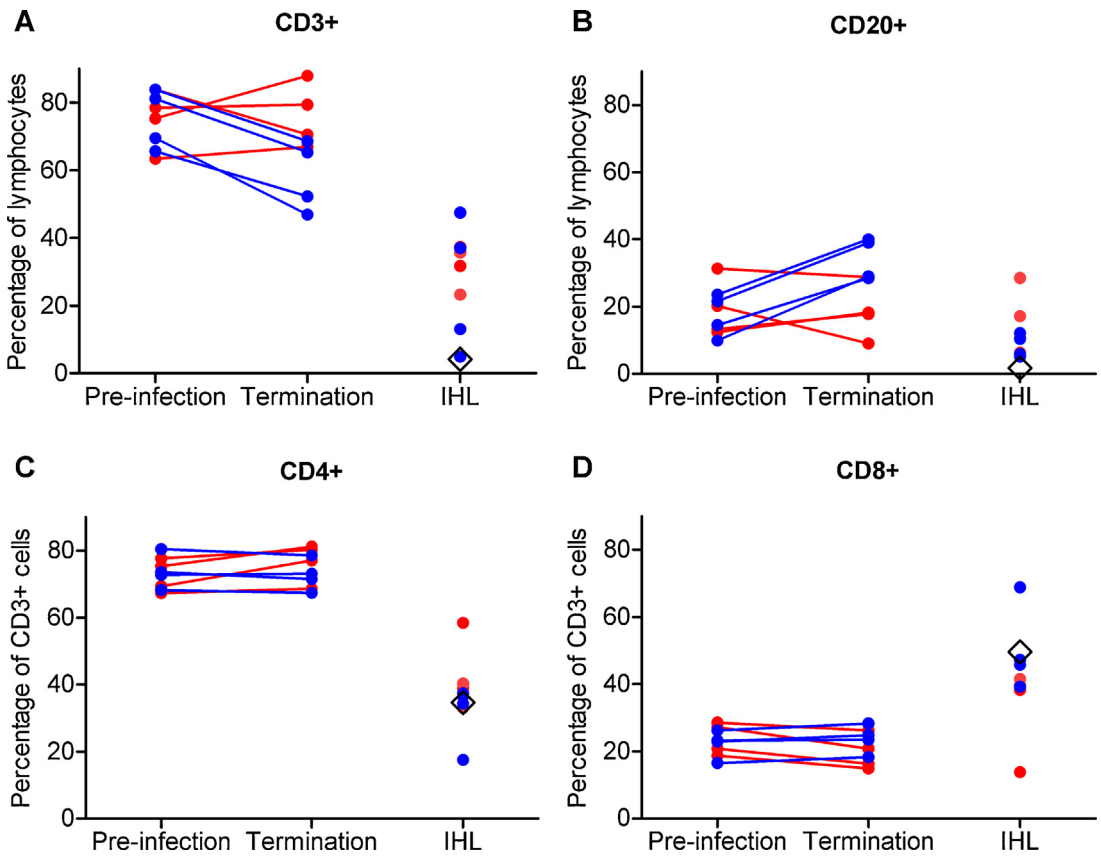

Fig. 2. Peripheral and hepatic lymphocyte dynamics during GBV-B infection of red-bellied tamarins. Percentage of lymphocyte fraction (as determined by forward scatter and side scatter characteristics) positive for (A) CD3 and (B) CD20. Percentage of $CD3^+$ fraction positive for (C) CD4 and (D) CD8. Animals are grouped according to the phase of infection at which they were sacrificed. Lymphocytes from a naive animal, G20, are represented by a black diamond.

decrease and one had a 10-fold decrease in the percentage of PD-1-expressing $CD4^+$ and $CD8^+$ T-cells. In the four tamarins that cleared infection there was a significant decrease in the percentage of PD-1-expressing $CD4^+$ T-cells and $CD8^+$ T-cells compared to pre-infection levels ($P < 0.001$). As several reports have indicated that the level of PD-1 expression may be a more informative indicator than absolute percentage of positive cells (Rutebemberwa et al., 2008; Shen et al., 2010; Vali et al., 2010), we determined the MFI for each population of T-cells. Trends for PD-1 expression level were comparable to those observed for percentages of positive cells, *i.e.* a significant reduction in PD-1 levels on $CD4^+$ ($P = 0.029$) and $CD8^+$ ($P = 0.004$) cells in convalescent tamarins relative to pre-infection levels (Fig. 3B).

Supplementary material related to this article can be found, in the online version, at http://dx.doi.org/10.1016/j.virusres.2013.11.006.

A distinct pattern of PD-1 expression was observed on IHL. Relative to IHL from a naive animal, $CD4^+$ T-cells from viremic tamarins displayed elevated PD-1 levels, both in percentage terms and relative expression level (Fig. 3C and D). In convalescent animals, PD-1 levels were significantly lower than during the viremic phase (absolute numbers, $P < 0.001$; relative expression level, $P = 0.029$) and approached those of the naive animal. PD-1 expression on $CD8^+$ IHL was largely unchanged from naive cells at either time of infection. However, only one naive sample was available for comparison, thus definitive baseline levels of PD-1 expression could not be established.

3.5. Histological analysis of liver tissue

Liver morphology in all tamarins was evaluated against a GBV-B-naive tamarin (Fig. 4A). Varying degrees of immune infiltration were observed around the portal tracts in all animals terminated at high viraemia (Fig. 4B–E). Marked immune infiltration was observed in two convalescent animals (W5 and V7) particularly around the portal tracts and within the sinusoids of the parenchyma, whereas W3 and V8 displayed levels of immune filtration similar to those of the naive animal (Fig. 4F–I).

3.6. Cellular immune responses against GBV-B NS3 in $CD3^+$ IHL

Sufficient IHL were available from six animals for analysis of cellular immunity. Responses against GBV-B NS3 were determined by intracellular cytokine staining of IFN-γ following peptide stimulation. A low frequency $CD4^+$ response to a single peptide pool was detected in one animal (W4) at high viraemia. An additional animal (V7) raised a $CD4^+$ response to a different peptide pool in the convalescent phase. $CD8^+$ T-cell responses were detected only in two convalescent animals (W5 and V7). Two responses were at low frequency; a third response was detected at high frequency (~15% of $CD8^+$ T-cells; Supplementary material, Fig. S2).

Supplementary material related to this article can be found, in the online version, at http://dx.doi.org/10.1016/j.virusres.2013.11.006.

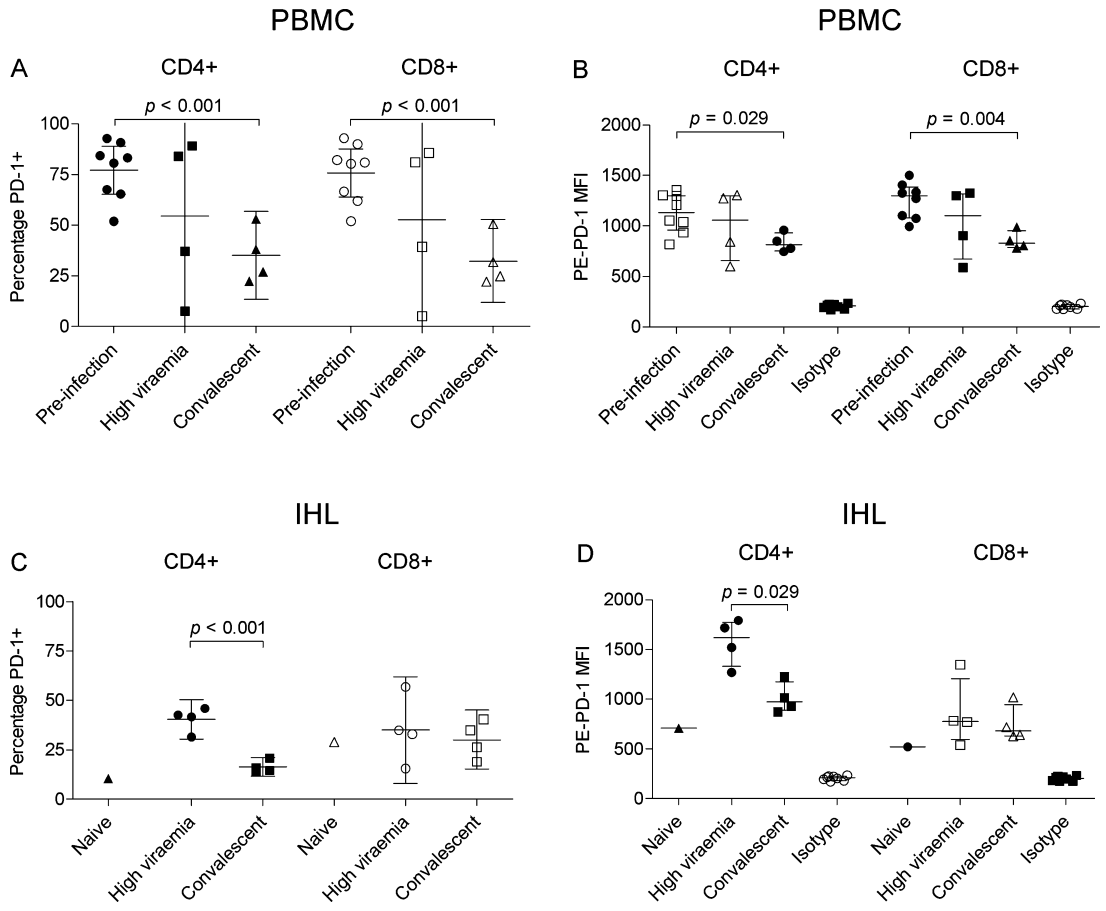

Fig. 3. Analysis of PD-1 expression on peripheral and intrahepatic CD3$^+$ lymphocytes from GBV-B-infected tamarins. (A and C) Proportion of CD4$^+$ and CD8$^+$ cells positive for PD-1 expression in PBMC and IHL prior to infection, during the viremic (6 wpi) and convalescent phase (24 wpi). (B and D) Median fluorescence intensity (MFI) of PE-PD-1 stained CD4$^+$ and CD8$^+$ populations. Naïve, cells from naive animal G20; Isotype, MFI of cells stained with PE-labelled isotype-matched control antibody; error bars indicate mean and 95% confidence intervals (left panels) or median and interquartile range (right panels). Significant differences between groups are indicated by relevant *p* values.

4. Discussion

Defining T-cell dynamics associated with the natural clearance of HCV is essential to understanding the key immune responses generated and so inform the development of effective anti-HCV immunotherapies and even prophylactic vaccines. The GBV-B tamarin model of acute viral hepatitis, can aid this investigation by allowing description of the phenotype of immune cell subsets post-infection and following natural clearance of a hepatotropic flavivirus, including direct analysis of the liver. Here we have defined T and B lymphocyte populations isolated not only from the periphery but also the liver at a period of high viraemia or in the subsequent convalescence period, when serum viraemia was undetectable. Surprisingly there was direct evidence of on-going virus replication in the liver. This observation has implications for understanding the immune responses involved not only in the initial clearance of acute hepacivirus infections but also the potential for establishment of chronic infection hitherto underestimated in this model.

Phenotyping of the peripheral lymphocyte population revealed that, in three of four animals terminated at 6 wpi with high viraemia, CD3$^+$ T-cell levels were greater than pre-infection levels reflecting an increase in the proportion of CD4$^+$ T-cells. While specificity of T-cells for antigens other than NS3 was not investigated due to limiting cell numbers this may correspond to the strong sustained multispecific peripheral CD4$^+$ T-cell response associated with the clearance of HCV in humans (Lechner et al., 2000; Chang et al., 2001; Thimme et al., 2001). A significant decrease in the percentage of peripheral CD3$^+$ T-cells compared with pre-infection samples coincided with a significant increase in the percentage of CD20$^+$ B-cells in the four tamarins terminated in the convalescence period. The increase in CD20$^+$ B-cells is consistent with reports of anti-NS3 antibody production peaking towards the end of infection and declining following clearance of viraemia (Beames et al., 2000; Martin et al., 2003).

Since the liver is the focal point of virus replication, we investigated changes in intrahepatic lymphocyte populations. In both high viremic and convalescent phases there was a greater percentage of CD3$^+$ T-cells and CD20$^+$ B-cells compared to the naïve tamarin. In contrast to marmosets (Jacob et al., 2004), the T-cell population comprised both CD4$^+$ and CD8$^+$ subsets that remained proportionally comparable to those in the uninfected animal. The magnitude of this increase was limited, however, in two convalescent animals (W5 and V7) in which the combined CD3$^+$ and CD20$^+$ population constituted <20% of the lymphocyte fraction. In both GBV-B-infected and uninfected tamarins a significant percentage of the IHL were CD3$^-$ CD20$^-$. There are reports of higher proportions of NK cells (which are CD3$^-$ CD20$^-$) in the liver than in the periphery of humans and mice (Crispe, 2003). Definitive identification of antibodies cross-reactive for tamarin CD16 and CD56 (as markers of NK cells) was not achieved therefore the phenotype of this population of cells could not be confirmed.

In a number of viral infections (Barber et al., 2006; Day et al., 2006) the failure to clear viraemia is associated with evidence of T cell exhaustion, while a single case of naturally resolving HCV infection was associated with a reversal of the exhausted phenotype (Raghuraman et al., 2012). We investigated PD-1 expression on

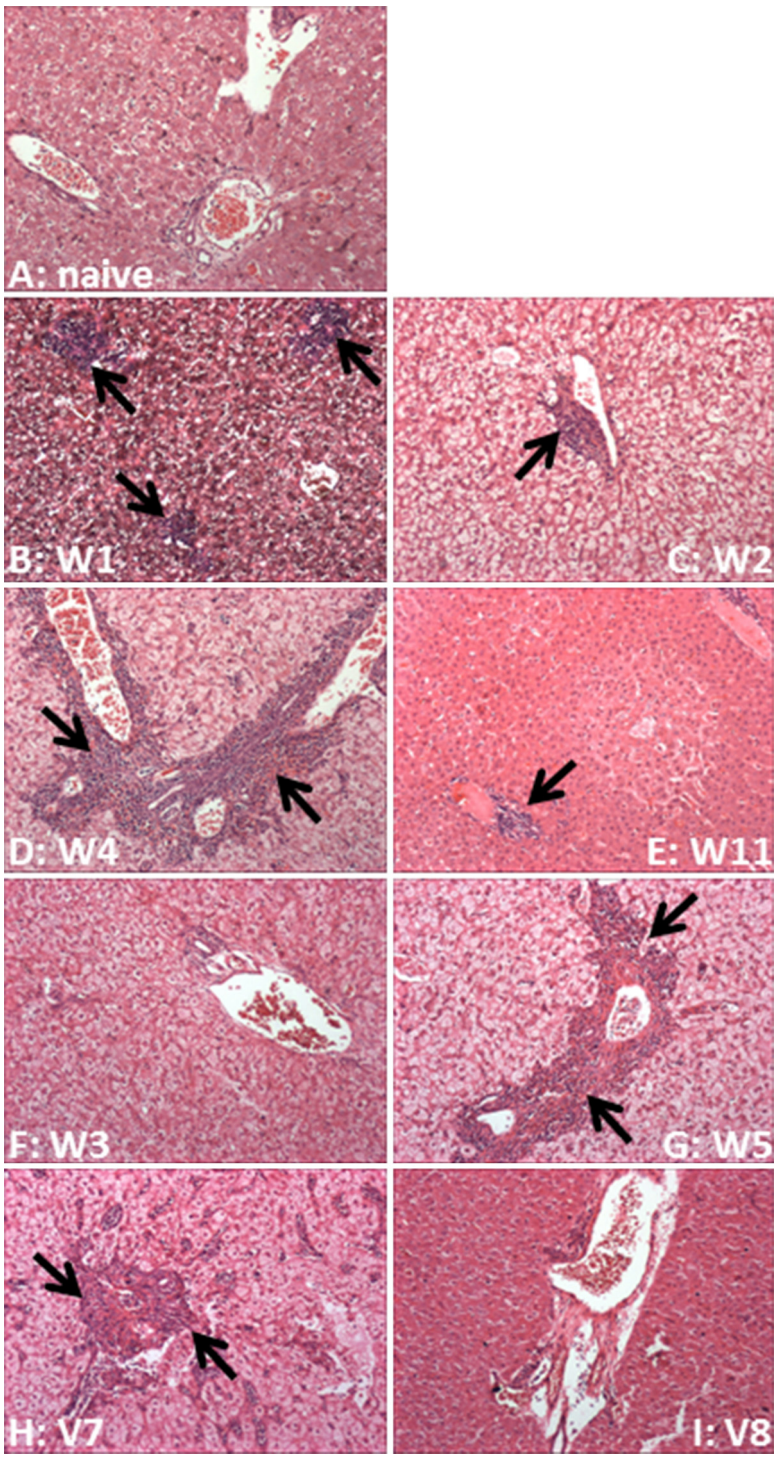

Fig. 4. Haematoxylin and eosin staining of liver tissue. (A) Naive tamarin; (B–E) tamarins terminated at high viraemia; (F–I) tamarins terminated at convalescence. Lymphoctye infiltration is indicated by arrows. Magnification 100×.

T-cells in GBV-B-infected tamarins to compare patterns of expression to those reported in acute HCV infection. The percentage of PD-1$^+$ CD4$^+$ cells and relative PD-1 expression levels in IHL were significantly higher in viremic animals than in naïve and convalescent animals. By contrast, PD-1 expression on CD8$^+$ T-cells was comparable between the two groups and was generally lower than on CD4$^+$ T-cells. Notably PD-1 expression patterns on intrahepatic CD4$^+$ T-cells appear typical of those seen on HCV-specific CD8$^+$ T-cells in the periphery in individuals that resolve HCV infection (Urbani et al., 2006; Kasprowicz et al., 2008; Nakamoto et al., 2008) but with higher levels of PD-1 on CD4$^+$ IHL rather than on CD8$^+$ IHL. While we have observed a GBV-B infection persisting in the periphery of a tamarin for 40 weeks (unpublished data), the limited number of animals with an infection reaching this stage currently precludes planned analysis of acute and long-term infections. Shin and colleagues studied intrahepatic PD-1 mRNA levels from HCV-infected chimpanzees (Shin et al., 2013) and found that while levels increased following infection, over the 28-week period of investigation little difference between the patterns of mRNA levels was noted between the two animals which controlled their infection

and the three that still had detectable viraemia at the end of the study. However, Rollier et al., reported elevated PD-1 mRNA levels in chronic infection in contrast to lower levels in the two animals which cleared infection, as noted in HCV infection (Rollier et al., 2007). Thus, a study whereby we could collate information from individual long-term GBV-B infections in tamarins would add to the description of the PD-1 levels in this model and in relation to HCV infection of humans.

The relatively low percentage of PD-1$^+$ CD4$^+$ and CD8$^+$ IHL from the naïve animal contrasts with the higher percentage of peripheral PD-1$^+$ T-cells pre-infection. PD-1 expression levels were markedly reduced in two tamarins with high viraemia, while all convalescent animals had significantly reduced PD-1 expression on both CD4$^+$ and CD8$^+$ T-cells. The mechanism underlying this reduction in PD-1$^+$ peripheral T-cells is unclear but may include recruitment of PD-1$^+$ cells to sites of viral replication or a more systemic down-regulation of PD-1 expression. The high percentage of PD-1$^+$ T-cells prior to infection was surprising given the low percentage of PD-1$^+$ T-cells in healthy humans (Vali et al., 2010). While it is possible that the antibody used is capable of detecting only high levels of PD-1, there are no identified alternatives that cross react with the tamarin homologue and it is expected to have a sufficient dynamic range to detect low levels of PD-1 as evidenced by the heterogeneous staining pattern seen on IHL (Supplementary Fig. 1C). A possible explanation stems from the fact that tamarins are often born as dizygotic twins and are natural bone marrow chimaeras (Watkins et al., 1990). A high level of PD-1 expression, as well as limited MHC polymorphism (Watkins et al., 1990, 1991; Mee et al., 2011) may play a role in the tolerance required. Future studies could employ an evaluation of PD-1 messenger RNA levels to further support the data.

The increase in the proportion of CD3$^+$ T-cells in the IHL of all animals suggests a role for a strong intrahepatic cell-mediated immune response in GBV-B clearance. Three of six tamarins produced a detectable response against NS3 though no pattern to the response was noted. The limiting numbers of IHL led us to employ pools of overlapping 20mer peptides, which may bind suboptimally to MHC class I molecules. Furthermore the low number of CD3$^+$ cells recovered in the IHL fraction limited the assay sensitivity thus some low-level responses may have been missed. Similarly, due to the limited volume of peripheral blood samples available to this study, an investigation of responses in the periphery was not possible. Due to a current limitation in availability of cross-reactive antibodies, only IFN-γ responses were investigated, though we recognise that CD4$^+$ T-cells in particular may be more likely to produce TNF-α and/or IL-2 in response to peptide stimulation. Hence, while our data are broadly consistent with the production of IFN-γ by marmoset IHL in response to NS3, NS4A and NS5B peptide stimulation (Woollard et al., 2008), and suggestive of a T-cell response, the intrahepatic T-cell responses likely extend beyond those described here. The identification of additional cross-reactive antibodies and immunodominant GBV-B epitopes could allow us to characterise more fully the immune response to the virus, building on these preliminary data.

Serum vRNA was undetectable in all four convalescent tamarins for at least 3 weeks prior to sacrifice. Immune infiltrate was clearly evident in two tamarins (W5 and V7), but far lower in the remaining two tamarins, implying recovery of normal liver morphology in these animals. Comparable staining patterns have been previously reported in GBV-B-infected animals (Karayiannis et al., 1989; Martin et al., 2003; Jacob et al., 2004) and were observed in the animals terminated at high viraemia. However, liver-associated GBV-B RNA was readily isolated and quantifiable by RT-PCR from all four convalescent animals, albeit to lower levels than those animals at the peak of infection. Hence, even at times when virus has apparently been 'cleared' from the blood, there is evidence of on-going virus replication in liver tissue which is further supported by evidence of immune activation in W5 and V7 observed at the same time point as the anti-NS3 response was detected. Our observations clearly indicate that apparent clearance of GBV-B from the periphery does not correlate with elimination of virus from the liver, a characteristic of other hepaciviruses where an occult infection underlines the persistent nature of infection. Such a reservoir of virus may provide the basis for recrudescence, as was observed in tamarin W5. However, it is not possible to definitively state that GBV-B has established an occult infection given the relatively short time span of this experiment: longer-term studies will be required to determine if liver-associated virus replicates at much later time points. Further, an investigation of the nature of the virus isolated to determine if it may be truly infectious would support the concept of establishment of an occult infection.

The immune response seen in W5 and V7 may be an effective response controlling infection or an example of a chronic immune response to low levels of virus that could cause secondary liver-associated pathologies, thus whether the tamarin immune response eradicates GBV-B or merely maintains viral replication at a low level warrants further investigation. The failure of the convalescent immune status to return to a pre-infection level may indicate that GBV-B is capable of establishing an occult infection. Further work is necessary, however, to determine the temporal association between clearance or persistence of virus in both the blood and the liver, and the liver pathology. Resolution of these questions will be an important issue for hepacivirus research with implications for HCV treatment and therapy.

5. Conclusion

Here we describe the dynamics of major lymphocyte populations at two time points in GBV-B infection of tamarins; high primary viremic phase and post-clearance of detectable viraemia. We observed a shift in the balance of CD3$^+$ and CD20$^+$ cells and tissue-specific alterations in expression of the activation/exhaustion marker PD-1. Critically, in the absence of peripheral viraemia, we have observed ongoing viral replication in the liver, which will impact on immunotherapy targeting for this and related viruses. A limited cellular immune response against GBV-B identified in the liver of tamarins supports the evidence of ongoing virus replication but further studies will be required to fully dissect the nature of this response. Future studies focusing on CD8$^+$ cytotoxic responses and CD4$^+$ proliferative responses will define the tamarin cell-mediated immune response against GBV-B. Our results provide a foundation for more detailed investigations of the acquired immune responses associated with elimination of flavivirus infection and add value to this surrogate model of HCV infection.

Competing interests

None of the authors declare any financial, personal, or professional interests that could be construed to have influenced the paper.

Authors' contributions

N.J.R., N.J.B., P.K., H.B. conceived and designed the experiments and analysed the data. S.P.H., E.T.M., H.P., O.B., J.M.D. performed and analysed the experiments. S.P.H. and N.J.R. wrote the paper. All authors edited and approved the final manuscript.

Acknowledgements

We gratefully acknowledge the expert assistance of veterinary and support staff and thank Jane Mitchell for preparing histological sections. Financial support was awarded by the UK Medical Research Council Grant number, G0900861 and EUPRIM-Net II, an EU FP7 grant. The funders had no role in study design, data collection and analysis, decision to publish, or preparation of the manuscript.

References

Barber, D.L., Wherry, E.J., Masopust, D., Zhu, B., Allison, J.P., Sharpe, A.H., Freeman, G.J., Ahmed, R., 2006. Restoring function in exhausted CD8T cells during chronic viral infection. Nature 439, 682–687.

Beames, B., Chavez, D., Guerra, B., Notvall, L., Brasky, K.M., Lanford, R.E., 2000. Development of a primary tamarin hepatocyte culture system for GB virus-B: a surrogate model for hepatitis C virus. J. Virol. 74, 11764–11772.

Beames, B., Chavez, D., Lanford, R.E., 2001. GB virus B as a model for hepatitis C virus. ILAR J. 42, 152–160.

Bowen, D.G., Walker, C.M., 2005. Adaptive immune responses in acute and chronic hepatitis C virus infection. Nature 436, 946–952.

Bright, H., Carroll, A.R., Watts, P.A., Fenton, R.J., 2004. Development of a GB virus B marmoset model and its validation with a novel series of hepatitis C virus NS3 protease inhibitors. J. Virol. 78, 2062–2071.

Bukh, J., Engle, R.E., Govindarajan, S., Purcell, R.H., 2008. Immunity against the GBV-B hepatitis virus in tamarins can prevent productive infection following rechallenge and is long-lived. J. Med. Virol. 80, 87–94.

Butkiewicz, N., Yao, N., Zhong, W., Wright-Minogue, J., Ingravallo, P., Zhang, R., Durkin, J., Standring, D.N., Baroudy, B.M., Sangar, D.V., Lemon, S.M., Lau, J.Y.N., Hong, Z., 2000. Virus-specific cofactor requirement and chimeric hepatitis C virus/GB virus B nonstructural protein 3. J. Virol. 74, 4291–4301.

Chang, K.M., Thimme, R., Melpolder, J.J., Oldach, D., Pemberton, J., Moorhead-Loudis, J., McHutchison, J.G., Alter, H.J., Chisari, F.V., 2001. Differential CD4(+) and CD8(+) T-cell responsiveness in hepatitis C virus infection. Hepatology 33, 267–276.

Chisari, F.V., 2005. Unscrambling hepatitis C virus-host interactions. Nature 436, 930–932.

Crispe, I.N., 2003. Hepatic T cells and liver tolerance. Nat. Rev. Immunol. 3, 51–62.

Day, C.L., Kaufmann, D.E., Kiepiela, P., Brown, J.A., Moodley, E.S., Reddy, S., Mackey, E.W., Miller, J.D., Leslie, A.J., DePierres, C., Mncube, Z., Duraiswamy, J., Zhu, B., Eichbaum, Q., Altfeld, M., Wherry, E.J., Coovadia, H.M., Goulder, P.J., Klenerman, P., Ahmed, R., Freeman, G.J., Walker, B.D., 2006. PD-1 expression on HIV-specific T cells is associated with T-cell exhaustion and disease progression. Nature 443, 350–354.

Heydtmann, M., Hardie, D., Shields, P.L., Faint, J., Buckley, C.D., Campbell, J.J., Salmon, M., Adams, D.H., 2006. Detailed analysis of intrahepatic CD8T cells in the normal and hepatitis C-infected liver reveals differences in specific populations of memory cells with distinct homing phenotypes. J. Immunol. 177, 729–738.

Hofmeyer, K.A., Jeon, H., Zang, X., 2011. The PD-1/PD-L1 (B7-H1) pathway in chronic infection-induced cytotoxic T lymphocyte exhaustion. J. Biomed. Biotechnol. (article ID 451694).

Jacob, J.R., Lin, K.C., Tennant, B.C., Mansfield, K.G., 2004. GB virus B infection of the common marmoset (Callithrix jacchus) and associated liver pathology. J. Gen. Virol. 85, 2525–2533.

Karayiannis, P., Petrovic, L.M., Fry, M., Moore, D., Enticott, M., McGarvey, M.J., Scheuer, P.J., Thomas, H.C., 1989. Studies of GB hepatitis agent in tamarins. Hepatology 9, 186–192.

Kasprowicz, V., Schulze Zur Wiesch, J., Kuntzen, T., Nolan, B.E., Longworth, S., Berical, A., Blum, J., McMahon, C., Reyor, L.L., Elias, N., Kwok, W.W., McGovern, B.G., Freeman, G., Chung, R.T., Klenerman, P., Lewis-Ximenez, L., Walker, B.D., Allen, T.M., Kim, A.Y., Lauer, G.M., 2008. High level of PD-1 expression on hepatitis C virus (HCV)-specific CD8+ and CD4+ T cells during acute HCV infection, irrespective of clinical outcome. J. Virol. 82, 3154–3160.

Lanford, R.E., Chavez, D., Notvall, L., Brasky, K.M., 2003. Comparison of tamarins and marmosets as hosts for GBV-B infections and the effect of immunosuppression on duration of viremia. Virology 311, 72–80.

Lechner, F., Wong, D.K., Dunbar, P.R., Chapman, R., Chung, R.T., Dohrenwend, P., Robbins, G., Phillips, R., Klenerman, P., Walker, B.D., 2000. Analysis of successful immune responses in persons infected with hepatitis C virus. J. Exp. Med. 191, 1499–1512.

Martin, A., Bodola, F., Sangar, D.V., Goettge, K., Popov, V., Rijnbrand, R., Lanford, R.E., Lemon, S.M., 2003. Chronic hepatitis associated with GB virus B persistence in a tamarin after intrahepatic inoculation of synthetic viral RNA. Proc. Natl. Acad. Sci. U.S.A. 100, 9962–9967.

Mee, E.T., Greenhow, J., Rose, N.J., 2011. Characterisation of Mhc class I and class II DRB polymorphism in red-bellied tamarins (*Saguinus labiatus*). Immunogenetics 63, 619–626.

Nakamoto, N., Kaplan, D.E., Coleclough, J., Li, Y., Valiga, M.E., Kaminski, M., Shaked, A., Olthoff, K., Gostick, E., Price, D.A., Freeman, G.J., Wherry, E.J., Chang, K.M., 2008. Functional restoration of HCV-specific CD8T cells by PD-1 blockade is defined by PD-1 expression and compartmentalization. Gastroenterology 134, 1927–1937.

Nam, J.-H., Faulk, K., Engle, R.E., Govindarajan, S., St Claire, M., Bukh, J., 2004. In vivo analysis of the 3′ untranslated region of GB virus B after in vitro mutagenesis of an infectious cDNA clone: persistent infection in a transfected tamarin. J. Virol. 78, 9389–9399.

Raghuraman, S., Park, H., Osburn, W.O., Winkelstein, E., Edlin, B.R., Rehermann, B., 2012. Spontaneous clearance of chronic hepatitis C virus infection is associated with appearance of neutralizing antibodies and reversal of T-cell exhaustion. J. Infect. Dis. 205, 763–771.

Rijnbrand, R., Yang, Y., Beales, L., Bodola, F., Goettge, K., Cohen, L., Lanford, R.E., Lemin, S.M., Martin, A., 2005. A chimeric GB virus B with 5′ nontranslated RNA sequence from hepatitis C virus causes hepatitis in tamarins. Hepatology 41, 986–994.

Rollier, A.C., Paranhos-Baccala, G., Verschoor, E.J., Verstrepen, B.E., Drexhage, J.A., Fagrouch, Z., Berland, J.L., Komurian-Pradel, F., Duverger, B., Himoudi, N., Staib, C., Meyr, M., Whelan, M., Adams, V.C., Larrea, E., Riezu, J.I., Lasarte, J.J., Bartisch, B., Cosset, F.L., Spaan, W.J., Diepolder, H.M., Pape, G.R., Sutter, G., Inchauspe, G., Heeney, J.L., 2007. Vaccine-induced early control of hepatitis C virus infection in chimpanzees fails to impact on hepatic PD-1 and chronicity. Hepatology 45, 602–613.

Rutebemberwa, A., Ray, S.C., Astemborski, J., Levine, J., Liu, L., Dowd, K.A., Clute, S., Wang, C., Korman, A., Sette, A., Sidney, J., Pardolol, D.M., Cox, A.L., 2008. High-programmed death-1 levels on hepatitis C virus-specific T cells during acute infection are associated with viral persistence and require preservation of cognate antigen during chronic infection. J. Immunol. 181, 8215–8225.

Shen, T., Zheng, J., Xu, C., Liu, J., Zhang, W., Lu, F., Zhuang, H., 2010. PD-1 expression on peripheral CD8+ TEM/TEMRA subsets closely correlated with HCV viral load in chronic hepatitis C patients. Virol. J. 7, 310.

Shin, E-C., Park, S-H., Nascimbeni, M., Major, M., Caggiari, L., de Re, V., Feinstone, S.M., Rice, C.M., Rehermann, B., 2013. The frequency of CD127+ hepatitis C virus (HCV)-specific T cells but not the expression of exhaustion markers predicts the outcome of acute HCV infection. J. Virol. 87, 4772–4777.

Stapleton, J.T., Foung, S., Muerhoff, A.S., Bukh, J., Simmonds, P., 2011. The GB viruses: a review and proposed classification of GBV-A, GBV-C (HGV), and GBV-D in genus Pegivirus within the family Flaviviridae. J. Gen. Virol. 92, 233–246.

Thimme, R., Oldach, D., Chang, K.M., Steiger, C., Ray, S.C., Chisari, F.V., 2001. Determinants of viral clearance and persistence during acute hepatitis C virus infection. J. Exp. Med. 194, 1395–1406.

Thimme, R., Bukh, J., Spangenberg, H.C., Wieland, S., Pemberton, J., Steiger, C., Govindarajan, S., Purcell, R.H., Chisari, F.V., 2002. Viral and immunological determinants of hepatitis C virus clearance, persistence, and disease. Proc. Natl. Acad. Sci. U.S.A. 99, 15661–15668.

Urbani, S., Amadei, B., Tola, D., Massari, M., Schivazappa, S., Missale, G., Ferrari, C., 2006. PD-1 expression in acute hepatitis C virus (HCV) infection is associated with HCV-specific CD8 exhaustion. J. Virol. 80, 11398–11403.

Vali, B., Jones, R.B., Sakhdari, A., Sheth, P.M., Clayton, K., Yue, F.Y., Gyenes, G., Wong, D., Klein, M.B., Saeed, S., Benko, E., Kovacs, C., Kaul, R., Ostrowski, M.A., 2010. HCV-specific T cells in HCV/HIV co-infection show elevated frequencies of dual Tim-3/PD-1 expression that correlate with liver disease progression. Eur. J. Immunol. 40, 2493–2505.

Watkins, D.I., Chen, Z.W., Hughes, A.L., Hodi, F.S., Letvin, N.L., 1990. Genetically distinct cell populations in naturally occurring bone marrow-chimeric primates express similar MHC class I gene products. J. Immunol. 144, 3726–3735.

Watkins, D.I., Garber, T.L., Chen, Z.W., Toukatly, G., Hughes, A.L., Letvin, N.L., 1991. Unusually limited nucleotide sequence variation of the expressed major histocompatibility complex class I genes of a New World primate species (*Saguinus oedipus*). Immunogenetics 33, 79–89.

Woollard, D.J., Haqshenas, G., Dong, X., Pratt, B.F., Kent, S.J., Gowans, E.J., 2008. Virus-specific T-cell immunity correlates with control of GB virus B infection in marmosets. J. Virol. 82, 3054–3060.

Yao, Z.Q., King, E., Prayther, D., Yin, D., Moorman, J., 2007. T cell dysfunction by hepatitis C virus core protein involves PD-1/PDL-1 signaling. Viral. Immunol. 20, 276–287.